Hindawi
Advances in Polymer Technology
Volume 2022, Article ID 6568456, 10 pages
https://doi.org/10.1155/2022/6568456

Research Article

Design and Optimization of Fuel Cells: A Case Study on Polymer Electrolyte Membrane Fuel Cell Power Systems for Portable Applications

Mehmet Fatih Orhan,[1] **Kenan Saka**,[2] **and Mohammad Yousuf**[1]

[1]*Department of Mechanical Engineering, College of Engineering, American University of Sharjah, P.O. Box 26666, Sharjah, UAE*
[2]*Vocational School of Yenisehir Ibrahim Orhan, Bursa Uludag University, P.O. Box 16900, Yenisehir, Bursa, Turkey*

Correspondence should be addressed to Mehmet Fatih Orhan; morhan@aus.edu

Received 2 March 2022; Revised 8 May 2022; Accepted 21 May 2022; Published 13 June 2022

Academic Editor: Yun Yu

Fuel cells are energy conversion devices that directly convert chemical energy of fuels such as hydrogen to useful work with negligible environmental impact and high efficiency. This study deals with thermodynamic analysis and modeling of polymer electrolyte membrane fuel cell (PEMFC) power systems for portable applications. In this regard, a case study of powering a computer with a PEMFC is presented. Also, an inclusive evaluation of various parameters such as voltage polarization, overall system efficiency, power output, and heat generation is reported. In addition, a parametric study is conducted to study the effect of many design and operation parameters on the overall efficiency. Results show the direct influence of current density and temperature values on optimization of the design parameters in PEMFCs.

1. Introduction

Global electricity generation is a main source of air pollution since it is mainly extracted from fossil fuels that lead to harmful emissions and their impacts on the environment. Power plants significantly contribute to the growing environmental problems such as global warming, regional acidification, and climate change [1]. In addition to environmental concerns, population growth, rising life standards, and depletion of fossil fuel lead to increase in energy price, which emerges the need for alternative fuels and energy conversion technologies that minimize the environmental impact along with high sustainability potentials.

Fuel cells are energy conversion devices that gained considerable attention lately for their potential to replace the conventional internal combustion engines and other energy conversion processes in power generation and transport applications. These electrochemical devices convert chemical energy of fuels such as hydrogen directly and efficiently into electricity through a simple reaction that yields only water and heat as by-products. This one-step generation of electricity in fuel cells replaces three steps of conventional power generation. First, fuel is burned in a combustion chamber to produce heat with greenhouse gases and pollution. Then, this heat is utilized in a heat engine to yield mechanical shaft work. Finally, the shaft work drives a generator that produces electrical power. Each of these conversion steps in the combustion chamber, heat engine, and generator sacrifice a portion of energy to reach a higher quality form, which eventually results in low overall conversion efficiency. Therefore, direct and simple conversions in fuel cells offer higher efficiency with less environmental impact. A cell consists of anode and cathode electrodes that sandwich an electrolyte in between. There are six common types of fuel cells, namely, alkaline fuel cell (AFC), proton exchange membrane fuel cell (PEMFC), direct methanol fuel cell (DMFC), molten carbonate fuel cell (MCFC), phosphoric acid fuel cell (PAFC), and solid oxide fuel cell (SOFC). Many cells are linked together to form a stack, which yields the desired current, voltage, and power outputs. Along with

their clean nature, high efficiency, immobility, durability, quiet, and reliable operations are among their many advantages [2–7].

The main issues hindering the further commercialization of fuel cells are the high cost and infrastructure. Therefore, there is an ongoing effort on design and optimization of fuel cells to improve their material and process performance and decrease the cost [8, 9]. For instance, a study by Hussain et al. [10] considered PEMFC in the application of light-duty fuel cell vehicle, in which many parameters were studied such as power output and efficiency at three different temperatures. A study by Kazim [11] conducted exergy analysis on PEMFC with different operation voltages. A different study by Cownden et al. [12] performed analysis of hydrogen fuel cell system for a bus transportation application. Their work addressed the irreversibilities in different system components. Sharaf and Orhan [13] conducted a comprehensive review on fuel cell technology and their recent impact on the market. Their work included a case study on a PEMFC system with various design and operational aspects, such as irreversibilities, power output, heat generation, and overall system efficiency. A PEMFC is studied by Grujicic and Chittajallu [14] using a single-phase two-dimensional electrochemical model. The optimum PEMFC design is found to be associated with the cathode geometrical and operation parameters which reduce the thickness of the boundary diffusion layer at the cathode/membrane interface. Liu et al. [15] have proposed a hybrid system for electric vehicle applications. The system consists of a PEMFC with a unidirectional DC/DC converter and a Li-ion battery stack with a bidirectional DC/DC converter. Also, in the system, the PEMFC is employed as the primary energy source, and the battery is employed as the second energy source. A model was developed by Kienitz [16] to examine the relationship between membrane thickness and vehicle range that takes into account anode purge rate. The model includes changes in efficiency and hydrogen utilization as a function of PEM thickness for a variety of operating conditions. Another model was used by Liu et al. [17] for the design optimization of fuel cells, which were fabricated and experimentally tested to compare the performance and examine these optimization effects. According to the study, a significantly higher power output was obtained from the fuel cell stack with optimized design of flow channels over that of without optimization.

Water and heat management are very crucial for the performance of PEMFCs. In this regard, response surface methodology (RSM) has been applied by Kahveci and Taymaz [18] to optimize these operation parameters of a PEMFC. It was concluded that the humidification and cell temperature are the basic factors affecting the power density of the fuel cell. The effect of polybenzimidazole in the electrode on the overall performance was studied by Parrondo et al. [19]. The electrochemical impedance measurements were in good agreement with the fuel cell polarization curves, and the optimum performance was obtained when overall resistance was minimal. Another one-dimensional model of a high-temperature PEMFC using polybenzimidazole (PBI) membranes was described by Mamlouk et al. [20]. The model simulated the influence of operating conditions, cell parameters, and fuel gas compositions on the cell voltage current density characteristics and also gave good predictions of the effect of oxygen and air pressures on cell behavior, and correctly simulated the mass transport behavior of the cell. A study of PEMFC end plate design by structural analysis was presented by Dey et al. [21]. They aimed to study the influence of cell geometry, bolt configuration, gasket thickness mismatch, and material properties of different components of average and distribution contact pressure. Hou et al. [22] have focused on a simplified finite element model for large PEMFC stack consisting of ten cells to investigate the internal structure deformation. The work provides important insight into the choice of the friction coefficient. According to Dhathathreyan et al. [23], air-breathing fuel cells have a great potential as power sources for various electronic devices. They reported the major advantage of the system as the reduced number of bipolar plates, and thereby, reduction in volume and weight. However, the thermal management was stated a challenge due to the nonavailability of sufficient air flow to remove the heat from the system during continuous operation.

The objective of this study is to present design and optimization of fuel cells via a case study of PEMFC powered computer. In this regard, the performance parameters such as voltage irreversibilities, losses, overall efficiency, power out, heat generation, and mass flow rates are evaluated. Also, a parametric study of the polarization curve at various operating conditions is carried out.

2. System Studied

Figure 1 shows a representation of the system via a flow diagram. The system includes a commercial PEMFC (Horizon H-500 XP Fuel Cell Stack) that supply a power value of 500 W. The stack has 30 cells, with an active area of 348.4 cm^2. It is air-cooled using an external cooling fan. It is a self-humidified fuel cell, without the use of any external humidification system [24]. The electrolyte in the cell consists of Nafion-112 with a land-to-channel ratio of 1 : 2.

At state 1 in Figure 1, pure hydrogen (H_2) fuel is supplied from a tank through a pressure regulator, to the fuel cell stack at ambient temperature and pressure. Commonly, fuel utilization factor is less than 1, which indicates that not all fuel is used in the anode, and this will require recirculation of the fuel for better fuel utilization and economy. Air is supplied in state 2 from atmosphere through an air filter to prevent dust and contaminations from entering the fuel cell and interfering with the gas diffusion layer (GDL). The air is supplied at atmospheric temperature and pressure. State 5 presents the output power through a cable supplied to the power supply of the laptop. The power supply is a conditioning device which adjusts the power supply to the laptop. State 6 represents the cooling air inlet to the system. Since the system is relatively small, water cooling is not necessary and air cooling through two external fans suffices the cooling requirement. PEMFC is free of hazards and the water coming out of state 7 is drinkable [25].

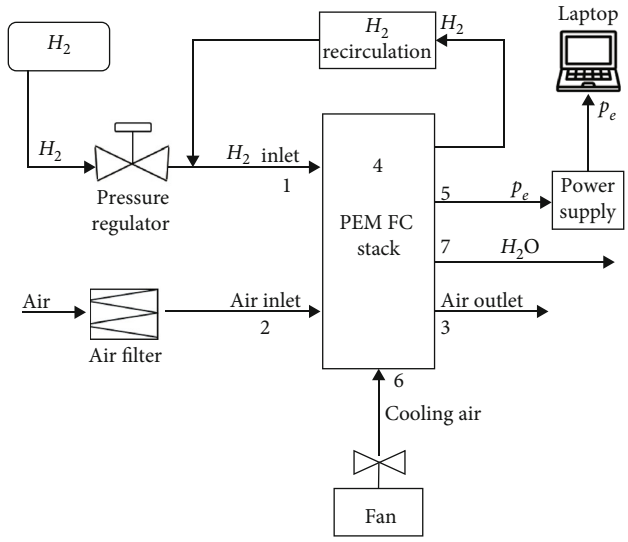

Figure 1: A flowchart of the PEMFC system to power a personal computer.

3. Analysis

Irreversible cell voltage losses or polarization is composed of activation polarization due to catalyst layers, fuel crossover losses due to fuel diffusion through the membrane into the cathode, ohmic polarization due to electron migration in the bipolar plates and electrode backing, proton migration in the polymer electrolyte membrane, and concentration overpotential due to the mass transfer limitations at higher current densities. The overall voltage polarization is determined through the following equation,

$$\Delta V_{\text{loss}} = \Delta V_{\text{act+cross}} + \Delta V_{\text{ohmic}} + \Delta V_{\text{concentration}}. \quad (1)$$

Activation polarization is due to the catalyst layers. It takes into account the electrochemical kinetics, and electron and proton migration, and is composed of both the anode and cathode catalyst layer activation polarization. Fuel crossover polarization occurs when some fuel diffuses from the anode through the electrolyte to the cathode and will lead to direct reaction with no electrical production. Fuel cross over losses are given by the following equation,

$$i_{\text{loss}} = \frac{2F\dot{n}_{H_2}}{A}, \quad (2)$$

where

$$\dot{n}_{H_2} = \frac{iA}{nF}. \quad (3)$$

The activation losses are determined through the following equation,

$$\Delta V_{\text{activation}} = \Delta V_{\text{anode}} + \Delta V_{\text{cathode}} = \frac{R_u T}{F}\left(\left(\frac{1}{\alpha_a}\ln\frac{i}{i_{o,a}}\right) + \left(\frac{1}{\alpha_c}\ln\frac{i}{i_{o,c}}\right)\right). \quad (4)$$

Since the anode activation losses is very small comparing to the cathode losses, the anode activation component is sometimes neglected. Therefore, combining equations (3) and (4), the following equation is obtained that describes the activation and fuel cross losses,

$$\Delta V_{\text{act+cross}} = \frac{R_u T}{F}\left(\left(\frac{1}{\alpha_c}\ln\frac{i_{\text{loss}} + i}{i_{o,c}}\right)\right). \quad (5)$$

Ohmic polarization is due to the resistance opposing electron motion through the cell. The components taken into account when calculating ohmic losses are anode resistance, electrolyte resistance, cathode resistance, and contact resistance.

$$\Delta V_{\text{ohmic}} = iA\sum R = iA\left(R_{\text{anode}} + R_{\text{electrolyte}} + R_{\text{cathode}} + R_{\text{contact}}\right),$$
$$\Delta V_{\text{ohmic}} = iA\left(\frac{L_a}{\sigma_a A} + \frac{L_e}{\sigma_e A} + \frac{L_c}{\sigma_c A} + \frac{R'_{\text{contact}}}{A}\right). \quad (6)$$

Concentration polarization is dominant at high current densities and occurs when the electrode reactions are hindered by reduced reactants availability at reaction sites. The concentration losses are given by the following equation,

$$\Delta V_{\text{concentration}} = \Delta V_{\text{anode}} + \Delta V_{\text{cathode}} = B_a \ln\left(1 - \frac{i}{i_{\text{lim},a}}\right) + B_c \ln\left(1 - \frac{i}{i_{\text{lim},c}}\right). \quad (7)$$

The voltage produced in a single cell is determined by subtracting the ideal case voltage V_o from the voltage polarization components as in the following equation,

$$V_c = V_o - \Delta V_{\text{act+cross}} - \Delta V_{\text{ohmic}} - \Delta V_{\text{concentration}} \quad (8)$$

The most important parameter in an energy study is the efficiency. The system efficiency considers the fuel cell efficiency with many factors such as fuel utilization, fuel reform efficiency, power conditioning efficiency, and balance of plant efficiency.

$$\eta_{\text{total}} = \frac{nFE}{\Delta H_f} \mu_{\text{fuel}} \eta_{pc} \eta_{\text{BoP}}, \quad (9)$$

where

$$\eta_{\text{BoP}} = 1 - a - \frac{b}{Ei}. \quad (10)$$

The power output of a single cell is obtained by multiplication of cell voltage with current, as in the equation,

$$P_c = V_c i A. \quad (11)$$

The power output of a total stack is obtained by multiplying the current with the voltage of stack, as in the equation:

$$P_e = V_c i A N. \quad (12)$$

Heat generation in PEMFCs is attributed to the conversion of some power to heat due to the irreversibilities discussed above. The heat generation is given [1] by $\dot{Q}_{\text{gen}} = P_e(V_o/V_c - 1)$. Assuming that only 40% of the heat generated by the fuel cell is removed by the air and the rest is radiated or naturally lost by convection from the outer surfaces, the rate of removal of heat by air is,

$$\dot{Q}_{\text{removal}} = 0.4 P_e \left(\frac{V_o}{V_c} - 1 \right). \quad (13)$$

Temperature is an important operational consideration for PEMFCs. Rising the temperature decreases the theoretical and reversible efficiency of the cell. Despite this theoretical indication, in reality, rising the temperature improves the fuel cell efficiency. This is due to the fact that at higher temperatures, the mass transfer within the fuel cell increases while the cell resistance drops. Hence, the polarization curve improves. However, the accumulation of product water in the oxidant stream limits operating temperatures to be below 100°C. At this temperature, water boils under 1 atm pressure, and its vapor reduces the partial pressure of oxygen in the air. As a result, the cell efficiency drastically decreases due to the oxygen starvation and can damage the fuel cell and reduce its lifespan. Also, membrane must be hydrated to conduct the protons. Hence, PEMFCs typically operate between 70 and 90°C. While the operation pressure can be increased to rise the boiling temperature of water, this raises other concerns and must be balanced accordingly in a proper stack design. The effect of the temperature can simply be given by the following Nernst equation,

$$E_{\text{nernst}} = -\frac{\Delta H - T\Delta S}{nF} + \frac{RT}{nF} \bullet \ln \frac{P_{H_2} P_{O_2}^{0.5}}{P_{H_2O}}. \quad (14)$$

It is important to also include a discussion about the effect of flow rates on the fuel cell efficiency when operation conditions are tackled. The amount of reactant gases consumed in a fuel cell is varied based on the current produced. Faraday's law describes the amount of gases that react in a fuel cell, in relation to the current,

$$itA = nzF, \quad (15)$$

where i, A, t, n, z, and F are the current density (A/cm^2), electrode area (cm^2), time (sec), number of moles, number of electrons in the reaction, and Faraday's constant, respectively. The formula can be further simplified to,

$$It = nzF, \quad (16)$$

where I is the current (A). According to the reactions that occur at the anode and the cathode, the flow rates of the reactant gases can be calculated as follows,

$$\dot{n}_{\text{hydrogen}} = \frac{I}{2F}, \qquad \dot{n}_{\text{oxygen}} = \frac{I}{4F}, \quad (17)$$

where $\dot{n}$ is the molar flow rate (mol/sec). It should be noted that the reactants are usually supplied in excess amount to the fuel cell. The ratio of the reactants at the cell inlet and its consumption rate is given by the stoichiometric effect as

$$S = \frac{N_{\text{supplied}}}{N_{\text{consumed}}}. \quad (18)$$

Typically, hydrogen is provided in excess ($S > 1$). As it flows through the stack, the unused gas is recirculated. Pure hydrogen is supplied at stoichiometric ratios between 1.1 and 1.2, while impure hydrogen requires higher ratios. For pure oxygen, the stoichiometric ratios are between 1.2 and 1.5, while the use of air requires stoichiometric ratios of 2 and above.

Mass flow rates depend on the current density required, for hydrogen supply, the mass flow rate is given by,

$$\dot{m}_{H_2} = 2.02x10^{-3} * \frac{I.N}{2F} = 1.05x10^{-8} * I * N. \quad (19)$$

For pure oxygen,

$$\dot{m}_{O_2} = 32x10^{-3} * \frac{I.N}{4F} = 8.29x10^{-8} * I * N. \quad (20)$$

Table 1: Design and operation parameters.

Parameter	Value	Unit	Description
α_a	0.5	—	Anode current transfer coefficient
α_c	0.6	—	Cathode current transfer coefficient
$i_{o,a}$	1.5	A/cm^2	Anode exchange current density
$i_{o,c}$	0.005	A/cm^2	Cathode exchange current density
A	348.4	cm^2	Active cell area
L_a	0.05	cm	Anode thickness
L_c	0.1	cm	Cathode thickness
L_e	0.51	cm	Electrolyte thickness
σ_a	2.49	S/m	Anode conductivity
σ_c	2.90	S/m	Cathode conductivity
σ_a	8.3	S/m	Electrolyte conductivity
R'_{contact}	0.03	Ω.cm^2	Total contact resistance
B_a	0.045	V	Anode empirical constant
B_c	0.045	V	Cathode empirical constant
$i_{\text{lim,a}}$	15	A/cm^2	Anode maximum current density
$i_{\text{lim,c}}$	2.5	A/cm^2	Cathode maximum current density
V_o	1.18	V	Reversible Nernst voltage at standard conditions
R_u	8.314	J/mol K	Universal gas constant
T	Varies	C^o	Operation temperature
n	2	—	Number of electrons transferred per mole
μ_{fuel}	0.95	—	Fuel utilization factor
η_{pc}	0.95	—	Efficiency of power conditioning devices
a	0.0499	W/m	BoP efficiency empirical constant
b	0.05	—	BoP efficiency empirical constant
ΔH_f	285,250	J/mol	Enthalpy of formation for PEM reaction
F	96485	C/mol	Faraday's constant
λ	1	—	Air stoichiometry

For air inlet,

$$\dot{m}_{\text{air,inlet}} = \lambda * \frac{28.97x10^{-3}}{0.21} * \frac{I.N}{4F} = 3.57x10^{-7} * I * N * \lambda. \quad (21)$$

For air exit,

$$\dot{m}_{\text{air,exit}} = \dot{m}_{\text{air,inlet}} - \dot{m}_{O_2}. \quad (22)$$

4. Results and Discussion

A case study on a PEMFC power system for a portable application (Figure 1) has been analyzed and optimized. The model in this study has been validated by experimental/theoretical results from the literature, including those in [10–12, 26] under various operating conditions.

The assumptions considered in this analysis are as follows: (1) the hydrogen storage cylinder is at constant pressure of 10 bar and temperature of 298°K; (2) 40% of the total heat generated by the stack are assumed to be removed by the air, and the rest is radiated or naturally lost by convection from the outer surfaces; and (3) the environment is at restricted state of STOP conditions, 298°K and 1 atm.

One of the main parameters evaluated in this study is the effect of operation temperature on various design parameters such as cell voltage, efficiency, and power output. For the equations presented earlier, four different data sets are extracted at four different temperatures (i.e., 10°C, 25°C, 50°C, and 100°C). The influence of operation temperature is significant in fuel cells. In the proposed application, the fuel cell operation environment can reach to 50°C, as in the case of summer season in United Arab Emirates. Designing for high temperatures allows good prediction of the results in extreme conditions. In analysis, the current density

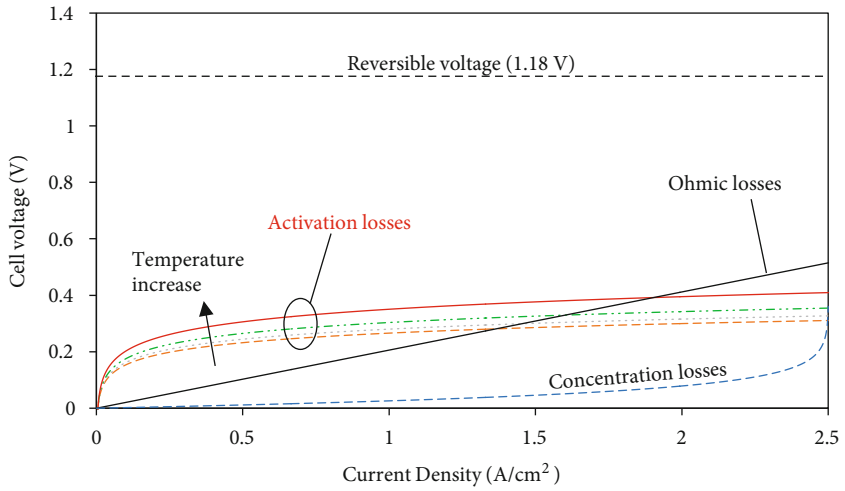

Figure 2: Voltage polarization curves for activation, ohmic, and concentration losses in the PEM FC stack.

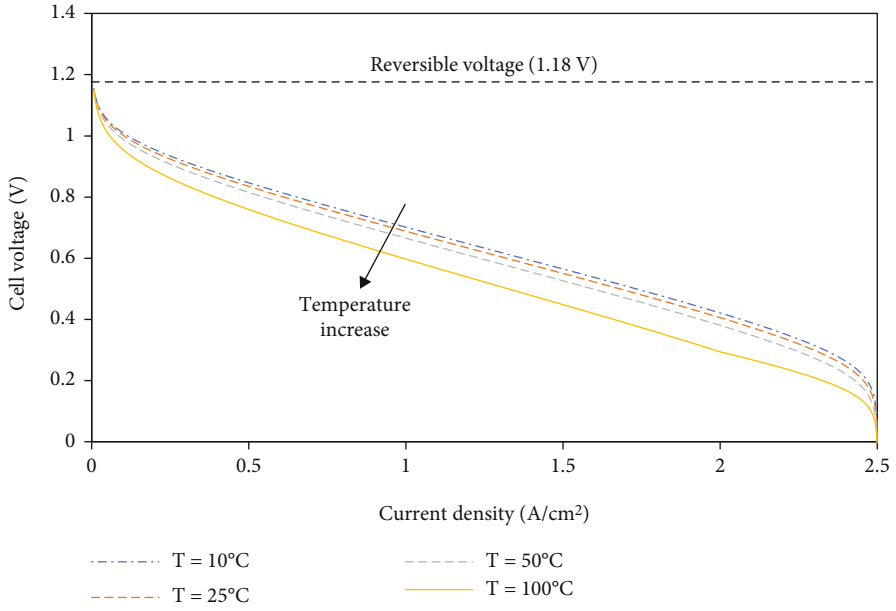

Figure 3: Variation of the cell voltage as a function of current density for different temperature values.

is varied in a range of 0 A/cm^2 to 2.5 A/cm^2. All constants, design, and operation parameters are described in detail in Table 1 with their respective values and units.

4.1. Voltage Polarization. Figure 2 presents the polarization curves of activation, ohmic, and concentration losses in a single cell as a function of current density *i*. Activation losses indicate a high loss at the beginning of the curve until a value of 0.5 A/cm^2, after which it starts assuming a lower effect. However, in concentration losses, an opposite trend is observed, as the loss is minimal at the beginning of the curve, and it starts showing a larger effect towards the end (typically after 2 A/cm^2). This is in accordance with the previous statement that concentration losses dominate at higher current density values. Ohmic losses show a linear behavior throughout the range. The losses decrease at higher temperatures, and the effect of temperature is dominant on the activation losses.

4.2. Cell Voltage. Figure 3 shows the variation of cell voltage as a function of current density for different temperature values. It can be observed that the temperature effect brings the curve downwards, which indicates a lower cell voltage at higher temperatures. The cell voltage curve exhibits rapid decrease at the start after which it behaves linearly and finally ending up decreasing rapidly. The linear region is of interest since it covers a large current density range, and it is easy to model using simple linear equations.

Figure 3 illustrates the effect of temperature on the theoretical voltage, due to the effect of temperature on the change

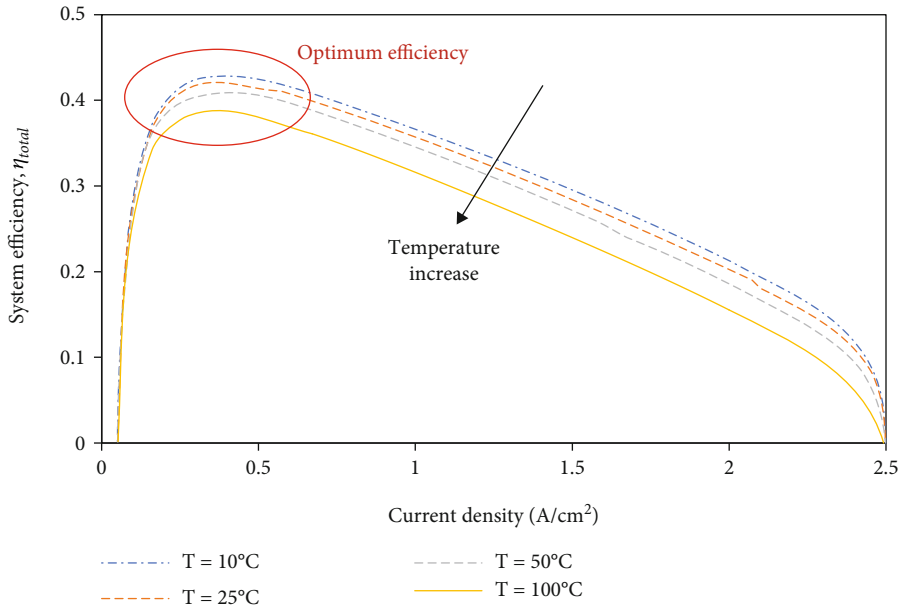

Figure 4: Overall cell efficiency of the PEM fuel cell system as a function of current density for different temperature values.

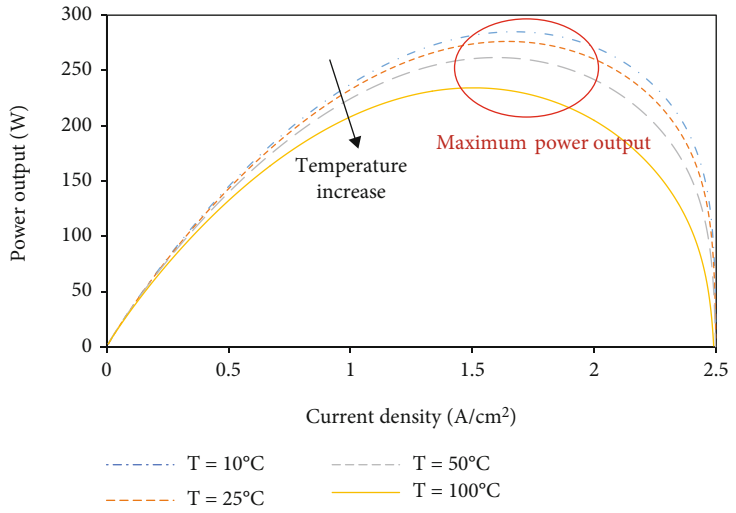

Figure 5: Cell power output as a function of current density for different temperature values.

in Gibbs free energy. However, the actual polarization curve at high temperatures may differ in working fuel cells due to the contradictory effects on mass transport and the decrease in the activation and ohmic losses. Even though Gibbs free energy change drops at high temperatures, cell losses decrease resulting in a higher efficiency. It is also observed that preheating and humidifying the reactants highly improve the cell efficiency especially at low current densities.

Fuel cell applications may have different operating conditions based on the system requirements. The common operating temperature range of PEMFCs is between 40 and 85°C. The lower operating temperatures provide quick start-up and enhance power density. On the other hand, the low operating temperature makes it more difficult to reject heat to the surroundings due to lower temperature differences. Hence, for automotive applications, higher operating temperatures are required for better efficiency. Additionally, higher temperatures also improve tolerance of the fuel cell to impurities such as carbon monoxide. This is especially necessary for any fuel cell operating on hydrocarbon reformates and impure hydrogen. While majority of PEMFCs operate at low-temperature ranges, a stationary power plant might benefit from a high operating temperature to use excess heat for cogeneration purposes. It is vital to obtain a proper energy and consequently humidity balances for a fuel cell. High temperatures can result in water evaporation within the membrane, which results in dehydration and low proton transport. On the other hand, very low temperatures can cause freezing and again efficiency degradation. This crucial task is especially difficult since the operation temperature of a fuel cell is

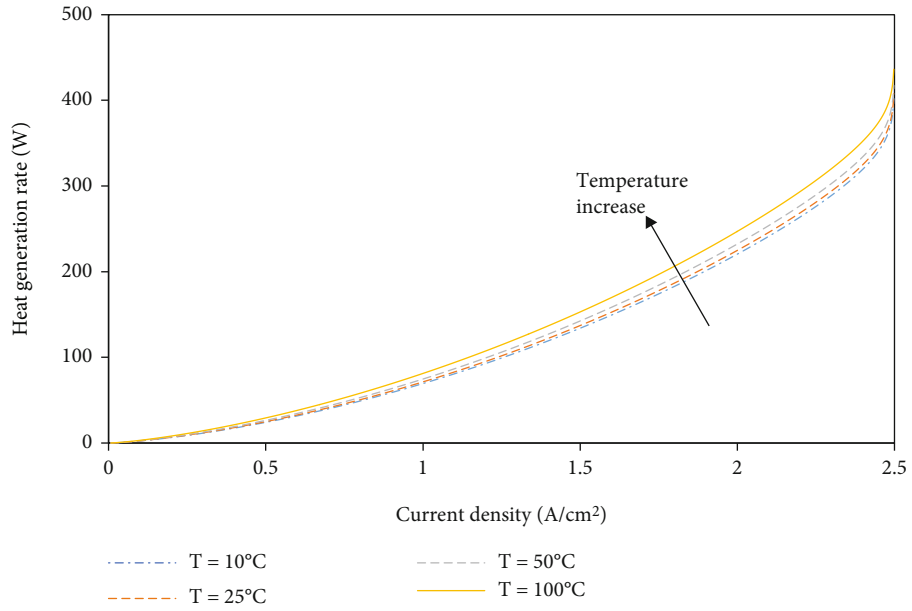

Figure 6: Heat generation as a function of current density for different temperature values.

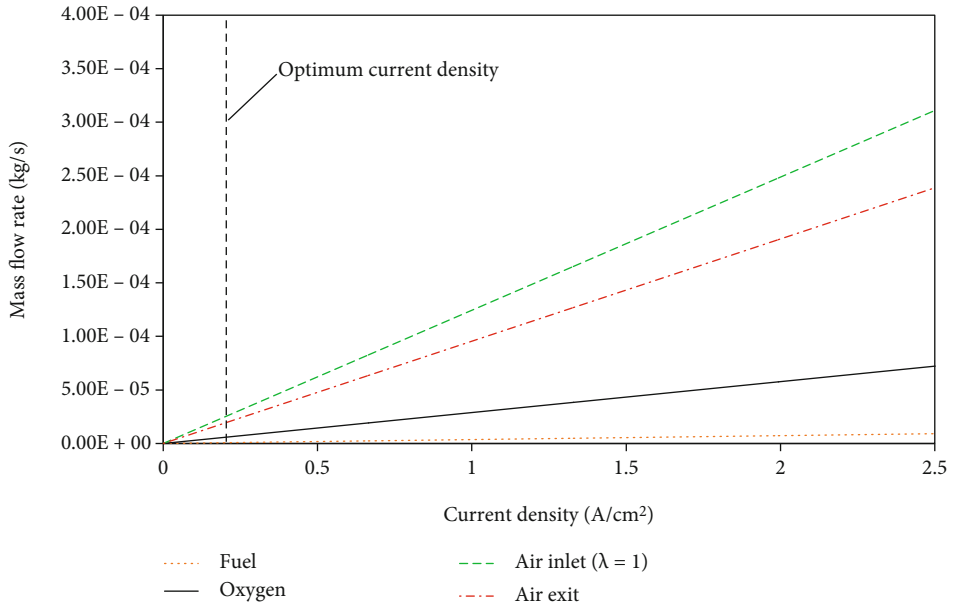

Figure 7: Mass flow rate of reactants as a function of current density.

formed by many parameters such as pressure, humidity, and condition of the reactants. Fuel cells are usually cooled by naturally breathing, air cooling fans, or liquid/water cooling systems that are suggested for systems above 100 W. Better cooling leads to a lower operation temperature, which yields better water management and humidity control that result in a higher performance.

4.3. Overall Efficiency. The overall efficiency of the system is represented in Figure 4. It is noted that the efficiency increases rapidly at the start as the current density rises, reaching a maximum value of 0.42 at current density of 0.35 A/cm^2. Similar to cell voltage curves, the efficiency exhibits a linear region in between current densities of 0.5 and 2 A/cm^2. This allows for a linear curve fitting when it comes to experimental data measurements. It is observed from the efficiency curve that it is possible to select an optimum design parameter such that the performance is within the maximum efficiency region. Temperature effect decreases the theoretical cell voltage, and therefore, the theoretical efficiency is decreased as observed.

4.4. Power Output. Cell power output as a function of current density for different temperature values is shown in

Figure 5. It can be observed that at a current density value of 1.75 A/cm^2, the net power produced by the cell is around 285 W. Also, the higher temperatures result in a lower power output since the power output is a function of cell voltage.

4.5. Heat Generation. The heat generated by the irreversibilities of the PEM fuel cell system is plotted in Figure 6. The rate of heat generation is low at low current density values, and it starts increasing rapidly towards the end of the current density range. This is attributed to the behavior of cell voltage in Figure 2, since the heat generation is inversely related to the cell voltage output. Therefore, the figure indicates an increase in heat generation at higher temperatures.

4.6. Mass Flow Rates. Mass flow rates of fuel and air as a function of current density are plotted in Figure 7. The behavior of mass flow rates is linear for all reactants, with higher values of air at cathode side. At a current density value of 0.35 A/cm^2, the mass flow rate values of fuel, oxygen, air inlet, and air outlet are 1.28×10^{-6}, 1.01×10^{-5}, 4.34×10^{-5}, and 3.32×10^{-5} kg/s, respectively.

5. Conclusions

In this study, an extensive performance analysis of a PEM fuel cell system to power a computer has been performed by evaluating various parameters such as cell irreversibilities, overall system efficiency, power output, heat generation, and mass flow rates. It can be concluded that the voltage polarization and its careful evaluation is crucial as it determines the cell performance and its power output. Improving the overall system efficiency requires a careful optimization of design and operation parameters. The temperature plays an important role in the behavior of many design parameters and must be considered when designing for any application. The design and performance analysis in this study can assist the ongoing efforts to understand the cell losses and consequently improve the overall performance of the PEMFC stacks.

Nomenclature

$\dot{n}$: Molar flow rate
ΔG: Gibbs free energy change
ΔS: Entropy change
ΔV: Voltage drop due to losses
A: Electrode area
B: Empirical constant
BoP: Balance of Plant
F: Faraday's constant
H: Enthalpy
i: Current density
I: Current
L: Length
n: Number of moles
N: Number of cells within the stack
P: Pressure
Q: Heat rate
R: Ideal gas constant
r: Internal resistance
R: Electrical resistance
S: Stoichiometric ratio
T: Temperature
t: Time
V: Cell voltage
z: Number of electrons
α: Transfer coefficient
σ: Electron conductivity

Subscripts and Superscripts

atm: Atmosphere
H: Hydrogen
nernst: Nernst equation
O: Oxygen

Abbreviations

GDL: Gas diffusion layer
HHV: Higher heating value
ICE: Internal combustion engine
LHV: Lower heating value
MEA: Membrane electrode assembly
OCV: Open circuit voltage
PEM: Polymer electrolyte membrane.

Data Availability

The data used to support the findings of this study are included within the article.

Conflicts of Interest

The authors declare that they have no conflicts of interest.

Acknowledgments

The work in this paper was supported, in part, by the Open Access Program from the American University of Sharjah. This paper represents the opinions of the author(s) and does not mean to represent the position or opinions of the American University of Sharjah.

References

[1] A. L. Dicks and D. A. J. Rand, *Fuel Cell Systems Explained*, Wiley, 2018.

[2] T. R. Ralph, G. A. Hards, J. E. Keating et al., "Low cost electrodes for proton exchange membrane fuel cells: performance in single cells and Ballard stacks," *Journal of the Electrochemical Society*, vol. 144, no. 11, pp. 3845–3857, 1997.

[3] H. Liu, C. Song, L. Zhang, J. Zhang, H. Wang, and D. P. Wilkinson, "A review of anode catalysis in the direct methanol fuel cell," *Journal of Power Sources*, vol. 155, no. 2, pp. 95–110, 2006.

[4] J. H. Wee, K. Y. Lee, and S. H. Kim, "Fabrication methods for low-Pt-loading electrocatalysts in proton exchange membrane fuel cell systems," *Journal of Power Sources*, vol. 165, no. 2, pp. 667–677, 2007.

[5] P. Costamagna and S. Srinivasan, "Quantum jumps in the PEMFC science and technology from the 1960s to the year 2000: part II. Engineering, technology development and application aspects," *Journal of Power Sources*, vol. 102, no. 1-2, pp. 253–269, 2001.

[6] K. Sopian and W. R. W. Daud, "Challenges and future developments in proton exchange membrane fuel cells," *Renewable Energy*, vol. 31, no. 5, pp. 719–727, 2006.

[7] L. Zhang, J. Zhang, D. P. Wilkinson, and H. Wang, "Progress in preparation of non-noble electrocatalysts for PEM fuel cell reactions," *Journal of Power Sources*, vol. 156, no. 2, pp. 171–182, 2006.

[8] C. Haynes and W. J. Wepfer, "Enhancing the performance evaluation and process design of a commercial-grade solid oxide fuel cell via exergy concepts," *Journal of Energy Resources Technology*, vol. 124, no. 2, pp. 95–104, 2002.

[9] I. Dincer, "Technical, environmental and exergetic aspects of hydrogen energy systems," *International Journal of Hydrogen Energy*, vol. 27, no. 3, pp. 265–285, 2002.

[10] M. M. Hussain, J. J. Baschuk, X. Li, and I. Dincer, "Thermodynamic analysis of a PEM fuel cell power system," *International Journal of Thermal Sciences*, vol. 44, no. 9, pp. 903–911, 2005.

[11] A. Kazim, "Exergy analysis of a PEM fuel cell at variable operating conditions," *Energy Conversion and Management*, vol. 45, no. 11-12, pp. 1949–1961, 2004.

[12] R. Cownden, M. Nahon, and M. A. Rosen, "Exergy analysis of a fuel cell power system for transportation applications," *Exergy, An International Journal*, vol. 1, no. 2, pp. 112–121, 2001.

[13] O. Z. Sharaf and M. F. Orhan, "An overview of fuel cell technology: fundamentals and applications," *Renewable and Sustainable Energy Reviews*, vol. 32, pp. 810–853, 2014.

[14] M. Grujicic and K. M. Chittajallu, "Design and optimization of polymer electrolyte membrane (PEM) fuel cells," *Applied Surface Science*, vol. 227, no. 1-4, pp. 56–72, 2004.

[15] J. Liu, Y. Zhao, B. Geng, and B. Xiao, "Adaptive second order sliding mode control of a fuel cell hybrid system for electric vehicle applications," *Mathematical Problems in Engineering*, vol. 2015, Article ID 370424, 15 pages, 2015.

[16] B. Kienitz, "Optimizing polymer electrolyte membrane thickness to maximize fuel cell vehicle range," *International Journal of Hydrogen Energy*, vol. 46, no. 19, pp. 11176–11182, 2021.

[17] H. Liu, P. Li, and K. Wang, "Optimization of PEM fuel cell flow channel dimensions–mathematic modeling analysis and experimental verification," *International Journal of Hydrogen Energy*, vol. 38, no. 23, pp. 9835–9846, 2013.

[18] E. E. Kahveci and I. Taymaz, "Experimental investigation on water and heat management in a PEM fuel cell using response surface methodology," *International Journal of Hydrogen Energy*, vol. 39, no. 20, pp. 10655–10663, 2014.

[19] J. Parrondo, C. V. Rao, S. L. Ghatty, and B. Rambabu, "Electrochemical performance measurements of PBI-based high-temperature PEMFCs," *International Journal of Electrochemistry*, vol. 2011, Article ID 261065, 8 pages, 2011.

[20] M. Mamlouk, T. Sousa, and K. Scott, "A high temperature polymer electrolyte membrane fuel cell model for reformate gas," *International Journal of Electrochemistry*, vol. 2011, Article ID 520473, 18 pages, 2011.

[21] T. Dey, J. Deshpande, D. Singdeo, and P. C. Ghosh, "Study of PEM fuel cell end plate design by structural analysis based on contact pressure," *Journal of Energy*, vol. 2019, Article ID 3821082, 11 pages, 2019.

[22] Y. Hou, L. Wang, J. Zhang, and D. Hao, "Effect of friction coefficient on relative slippage of fuel cell stack under mechanical impact condition," *Modelling and Simulation in Engineering*, vol. 2018, Article ID 1843071, 8 pages, 2018.

[23] K. S. Dhathathreyan, N. Rajalakshmi, K. Jayakumar, and S. Pandian, "Forced air-breathing PEMFC stacks," *International Journal of Electrochemistry*, vol. 2012, Article ID 216494, 7 pages, 2012.

[24] F. C. Store, *Horizon XP PEM Fuel Cell 500W*https://www.fuelcellstore.com/fuel-cell-stacks/medium-power-fuel-cell-stacks/horizon-h500-xp-pemfc.

[25] V. Ovsiankin, *Toyota Mirai, DRINK?*, 2015, https://www.youtube.com/watch?v=ex1NZ8-bXvg.

[26] J. H. Jang, H. C. Chiu, W. M. Yan, and W. L. Sun, "Effects of operating conditions on the performances of individual cell and stack of PEM fuel cell," *Journal of Power Sources*, vol. 180, no. 1, pp. 476–483, 2008.